AGU PUBLICATIONS

JGR

Journal of Geophysical Research: Atmospheres

RESEARCH ARTICLE
10.1002/2015JD023508

Key Points:
- Why SGP drought occurs in some La Niña years but not others is examined
- Anomalous positive TNA in spring and negative NAO in summer favor SGP droughts
- The influence of Niño 3.4 SST is only significant in winter

Correspondence to:
B. Pu,
bing.pu@noaa.gov

Citation:
Pu, B., R. Fu, R. E. Dickinson, and D. N. Fernando (2016), Why do summer droughts in the Southern Great Plains occur in some La Niña years but not others?, *J. Geophys. Res. Atmos.*, *121*, doi:10.1002/2015JD023508.

Received 10 APR 2015
Accepted 31 DEC 2015
Accepted article online 5 JAN 2016

Why do summer droughts in the Southern Great Plains occur in some La Niña years but not others?

Bing Pu[1], Rong Fu[1], Robert E. Dickinson[1], and D. Nelun Fernando[2]

[1]Department of Geological Sciences, Jackson School of Geosciences, University of Texas at Austin, Austin, Texas, USA, [2]Texas Water Development Board, Austin, Texas, USA

Abstract Droughts in the Southern Great Plains (SGP) have been attributed to the cold phase of El Niño–Southern Oscillation or La Niña. While La Niña events have been clearly linked to winter droughts, their link to summer droughts has remained unclear. We analyze the difference in precipitation between dry and nondry summers over the SGP during La Niña years. Anomalously high geopotential height and subsidence over the SGP occur in spring, along with an intensified northward moisture flux that advects moisture away to the northern plains and Midwest. The dependence of SGP drought on La Niña is statistically significant only in winter and becomes insignificant in spring and summer. The drought development in La Niña years is related to an anomalous warming over the tropical North Atlantic in spring and an anomalous negative North Atlantic Oscillation (NAO) in summer, both of which suppress precipitation by strengthening the anomalous high over the SGP and displacing the subtropical jet streams. In years with relatively large precipitation anomalies (i.e., the 27% driest and wettest La Niña years over the SGP), up to 45% of the variances of summer precipitation can be explained by a linear combination of the Niño 3.4 sea surface temperature (SST), Pacific Decadal Oscillation (PDO), tropical North Atlantic SST, and NAO indices. An anomalously strong dry summer appears to be largely a result of a superposition of these factors.

1. Introduction

Drought is one of the most severe natural disasters as shown by the 1930s dust bowl, which reshaped the economy and society of the Great Plains [*Worster*, 1979], and the recent severe 2010–2011 drought over the Southern Great Plains (SGP) that caused about $12 billion in damage (http://www.ncdc.noaa.gov/billions/events.pdf).

Many efforts have been made to study and monitor the development of droughts and their underlying mechanisms. One such mechanism, La Niña, has long been related to drought in the Great Plains [e.g., *Trenberth et al.*, 1988; *Ting and Wang*, 1997; *Dai et al.*, 1998; *Schubert et al.*, 2004; *Seager et al.*, 2005a; 2005b; *Schubert et al.*, 2009; *Seager et al.*, 2014]. In cold seasons, its abnormal sea surface temperature (SST) and consequent diabatic heating excite wave trains from the tropical Pacific to North America, placing an anomalous high over the southern U.S., shifting the Pacific storm track northward, and consequently reducing precipitation over the Great Plains. For example, the 2010–2011 SGP drought has been related to a strong La Niña event during the winter and spring, along with other factors such as atmospheric internal variability [*Seager et al.*, 2014]. Such a tropical Pacific midlatitude teleconnection is less well established in summer, as the Rossby wave propagation can be trapped by tropical easterlies [e.g., *Ting and Wang*, 1997], although several studies have suggested a connection between El Niño and anomalous wet northern Great Plains in summer [e.g., *Wang et al.*, 2012] and a moderate relationship between El Niño and the Great Plains low-level jet during July–September [e.g., *Weaver et al.*, 2009; *Krishnamurthy et al.*, 2015].

However, La Niña is not always a good predictor of the droughts in the SGP. For example, the 1973–1975 La Niña event actually led to increased precipitation over the eastern Great Plains and Gulf coast, but climate models failed to reproduce this precipitation change, probably due to their strong sensitivity to the El Niño–Southern Oscillation (ENSO) [*Schubert et al.*, 2004; *Lau et al.*, 2006; *Seager and Hoerling*, 2014]. What factors could lead to such variability in precipitation during La Niña years? *Seager and Hoerling* [2014] have articulated that random atmosphere variability and other SST anomalies, e.g., of the tropical Atlantic and Indian Ocean, may overcome the influence of the tropical Pacific. This issue is examined here by seasons and in more detail in observations.

Modeling studies have found that combined cold pan-Pacific and warm Atlantic Multidecadal Oscillation (AMO) SST patterns would have stronger impact on droughts in the SGP than either alone. However, such modeled precipitation responses are less robust to a warm Atlantic sea surface temperature anomaly (SSTA) than that to a cold pan-Pacific SSTA [e.g., *Mo et al.*, 2009; *Schubert et al.*, 2009]. *Mo et al.* [2009] found that AMO played an indirect role in drought by modulating the impact of ENSO. On the other hand, *Nigam et al.* [2011] found in observations that northern Atlantic SSTs were important for the 1930s dust bowl and 1950s drought, accounting for up to 55% of the precipitation deficit observed in the latter. *Kushnir et al.* [2010] found that during the warm season (April–September), the influence of the tropical North Atlantic on U.S. precipitation (mainly in the SGP) per 1 standard deviation of SST anomaly is larger than that of ENSO. However, whether Atlantic SST anomalies could be responsible for the differences between dry and nondry La Niña years over the SGP has not been clear.

The SGP drought in the winter of 2010/2011 has also been related to the North Atlantic Oscillation (NAO) leading to mean flow divergence [*Seager et al.*, 2014]. *Ruiz-Barradas and Nigam* [2005] and *Weaver and Nigam* [2008] found that the NAO is linked to the variability of Great Plains low-level jet in summer, influencing onshore moisture transport, and thus precipitation in the Great Plains. Whether the NAO can also affect the occurrence of dry or nondry conditions during La Niña events has been unclear. Thus, we analyze the SST patterns and circulation conditions in the La Niña dry versus nondry years in the SGP from 1950 to 2013 to explore whether other SST anomalies or NAO can account for their differences in associated precipitation anomalies.

2. Methodology

2.1. Data Sets

To understand how circulation patterns and moisture convergence differ between La Niña dry and nondry years, winds, geopotential height, and specific humidity are analyzed from the National Centers for Environmental Prediction (NCEP)/National Center for Atmospheric Research (NCAR) reanalysis [*Kalnay et al.*, 1996, hereafter NCEP1] from 1948 to 2013. This reanalysis is chosen because of its long record. Its horizontal resolution is 2.5° by 2.5°.

The monthly precipitation of the Climatic Research Unit (CRU) TS3.21 [*Jones and Harris*, 2013] on a 0.5° latitude by 0.5° longitude grid from 1901 to 2012 is used to examine precipitation variations. These monthly precipitation data are gridded from station observations on daily or subdaily time scales. CRU TS3.21 used the same methodology as for its version TS 3.20 but with updated 2012 data and error corrections.

The Niño 3.4, Pacific Decadal Oscillation (PDO), and NAO indices from the NCEP Climate Prediction Center (CPC; http://www.esrl.noaa.gov/psd/data/climateindices/list/) are used. The monthly Niño 3.4 index is calculated from the extended reconstructed sea surface temperature (ERSST, v3b) [*Smith et al.*, 2008] averaged over the tropical Pacific between 5°N–5°S and 120°–170°W and is available from 1950 to present. The monthly standardized PDO index derived from the leading principal component of SST anomalies in the northern Pacific Ocean is available from 1948 to present. The NAO index normalized by its mean from 1981 to 2010 is available from 1950 to present.

The Hadley Centre sea ice and sea surface temperature (HadISST) data set [*Rayner et al.*, 2003] from the UK Met Office is used to examine SST patterns. Monthly SSTs on a 1° by 1° grid are available from 1870 to present. The Niño 3.4 index calculated from the HadISST is highly correlated (0.87) with the CPC Niño 3.4 index, and so the former is used to calculate regression and correlation patterns as it provides slightly longer time coverage than the CPC index. The tropical North Atlantic (TNA) SST index is calculated by averaging Atlantic SST between 0° and 20°N from the HadISST.

2.2. Criteria for La Niña Dry and Nondry Years

Three-month running mean ERSSTv3b SST anomalies in the Niño3.4 region from the CPC (http://www.cpc.ncep.noaa.gov/products/analysis_monitoring/ensostuff/ensoyears.shtml) are used to identify La Niña years from 1950 to 2013. Since we are interested in La Niña events that occur before or simultaneously with SGP summer precipitation anomalies, the occurrence of one of the following two criteria is used to decide the occurrence of such events: (i) During January–April (including December-January-February (DJF), January-February-March (JFM), February-March-April (FMA), and March-April-May (MAM)) at least three consecutive 3 month running means show negative SSTA greater than −0.5°C, or (ii) during May–August

Table 1. List of Dry and Nondry Years in the Southern Great Plains (SGP) With La Niña Signal From Winter to Summer (See Text for Details) From 1950 to 2013 Based On the Niño 3.4 Index From the NCEP Climate Prediction Center (CPC)[a]

	Years
All La Niña	1950, 1954–1956, 1964, 1968, 1970, 1971, 1973–1976, 1985, 1988, 1989,1996, 1998–2001, 2006, and 2008–2012
LaDry	2011, 1956, 1998, 1970, 2012, 1954, and 1964
LaNonDry	1950, 1975, 1989, 1968, 1996, 1999, and 1971

[a]"LaDry" and "LaNonDry" years are defined as the seven driest and wettest years from the total 26 La Niña years.

(including April-May-June (AMJ), May-June-July (MJJ), June-July-August (JJA), and July-August-September (JAS)) there are at least two consecutive running means showing negative SSTA greater than −0.5°C. Although our criteria are different from those of the CPC for the warm or cold episodes, the resultant La Niña years would still generally meet CPC's criteria if we had included November–December (i.e., October-November-December and November-December-January) from the previous year or extended to the fall of the same year as many La Niña events develop from fall or winter and last to late spring, while other events develop from summer and last to the end of the year or into the next year, e.g., 1970, 1998, and 2010. Twenty-six La Niña years are so identified during 1950–2013 (Table 1). Since 2013 is not a La Niña year and CRU TS3.21 precipitation data ends in 2012, our analysis considers the period 1950–2012.

To understand different precipitation responses during these La Niña events, dry and nondry composites, namely, LaDry and LaNonDry, are formed, corresponding to the seven (about 27%) driest and seven wettest May-June-July-August (MJJA) precipitation anomalies of the 26 La Niña years. The MJJA average is chosen because the total precipitation generally peaks from May to September with a mildly drier period in between, mainly contributed by the "midsummer drought" [e.g., *Magaña et al.*, 1999] in Mexico (Figure 1b), and MJJA precipitation contributes to about 44% of the total annual precipitation. The precipitation anomalies over the SGP also show strong persistence during this period.

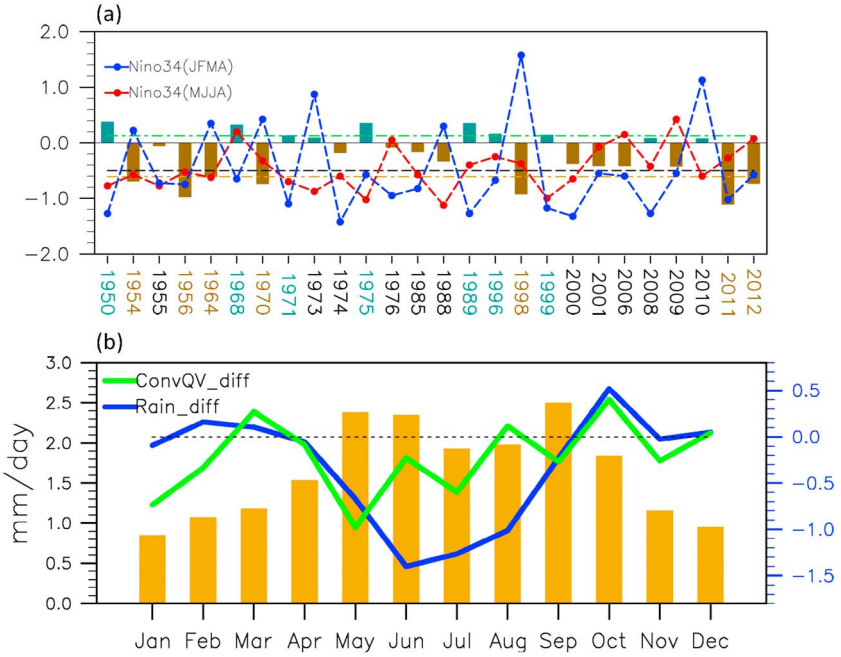

Figure 1. (a) Time series of La Niña years May-June-July-August (MJJA) precipitation (mm d^{-1}; turquoise and brown bars) averaged in the SGP (see the black box in Figure 2) along with CPC 3 month running mean Niño 3.4 SSTA (K) during JFMA (i.e., centered in JFMA; blue) and MJJA (red) from 1950 to 2012. −0.5 K is denoted by a black dashed line, ± 27% level of precipitation is denoted by green and brown dash dotted lines. The seven dry (nondry) years used in the composites are marked in brown (turquoise) in *x* axis. (b) Climatological monthly SGP precipitation (yellow bars) along with the differences of precipitation (blue; mm d^{-1}, right *y* axis) and vertically integrated (from surface pressure to 300 hPa) mass-weighted moisture convergence (green; mm d^{-1}, right *y* axis) between the LaDry and LaNonDry composites. Here monthly mean moisture convergence is shown but the daily transient contribution is not included.

2.3. Pattern Correlation

The pattern correlation, i.e., the Pearson product-moment coefficient, is used in section 3.3 to compare the spatial pattern of anomalous geopotential height in the NCEP1 reanalysis with the reconstructed height fields of the LaDry and LaNonDry composites and their differences. Here centered correlation is used, i.e., the spatial mean is removed, giving a better comparison of the pattern of height gradients. The height field in NCEP1 is denoted by X_{ij}, and the reconstructed field is Y_{ij}, where $i = 1, 2, 3, \ldots, n$ and $j = 1, 2, 3, \ldots, m$ are the latitude and longitude grids in the domain. The spatial means of X_{ij} and Y_{ij} are removed. The correlation coefficient r is calculated as the following:

$$r = \frac{\sum\left(\mathrm{WGT}_i X_{ij} Y_{ij}\right)}{\sqrt{\sum \mathrm{WGT}_i X_{ij}^2}\sqrt{\sum \mathrm{WGT}_i Y_{ij}^2}}, \tag{1}$$

where $\mathrm{WGT}_i = \cos(\mathrm{lat}(i))$ is an area weight and the sum is over the North Pacific-North America-North Atlantic region (5°S–75°N, 0°–180°W).

2.4. Bootstrap Test

The statistical significance of the differences between the LaDry and LaNonDry composites is examined by Bootstrapping resampling. First, two 7 year composites are randomly selected from the 26 La Niña years, and then the differences between the two composites are calculated. This process is repeated for 10,000 times to get the 5% and 95% levels for the differences. The differences between grid point values of the dry and nondry composites are considered significant at the 90% confidence level if they exceed these levels.

2.5. Collinearity of the Indices

We examined the Niño 3.4, PDO, TNA, and NAO indices to establish whether as predictors they are highly correlated with each other when used in multiple linear regressions. For this purpose, we calculated the variable inflation factor (VIF) [e.g., *Abudu et al.*, 2011]. A large value of VIF (usually 5–10) indicates one predictor can be largely explained by the other predictors, and thus the regression may be less reliable. Here the VIFs of these indices are all smaller than 2.1 during both the 26 La Niña years and from 1950 to 2012.

Previous studies [e.g., *Alexander et al.*, 2002] found that the cold tropical Pacific SSTA in winter would lead to cold tropical Atlantic SSTA in spring and summer. Although the VIFs among spring PDO, TNA, NAO, and winter Niño 3.4 indices are lower than 2.1, we also found a significantly positive (95% confidence level) correlation between the DJF Niño 3.4 index and MAM and JJA TNA indices, respectively, indicating that when the tropical Pacific is cold in winter, a cold SSTA is likely to develop in the tropical North Atlantic in the following spring and summer. More discussion on this issue is presented in section 3.2. Due to the correlations between the tropical Pacific and Atlantic SSTs, multiple linear regressions using both the TNA and Niño 3.4 indices are thus applied to precipitation, wind, geopotential height, and moisture flux fields when examining the teleconnection patterns associated with the TNA index (section 3.2). The patterns would be very similar to the linear regressions calculated by the TNA index alone if the influences of the Niño 3.4 index on the tropical North Atlantic SST were removed before calculating the TNA index.

2.6. Stationary and Transient Moisture Flux and Convergence

The total vertically integrated mass-weighted moisture flux ($-\int_{ps}^{ptop} \frac{q\vec{V}}{g} dp$) and moisture convergence ($\int_{ps}^{ptop} \frac{\nabla\left(q\vec{V}\right)}{g} dp$) are calculated from daily data of the NCEP1 reanalysis. We use p_s and p_{top} to denote the bottom and top pressure layers, i.e., surface pressure and 300 hPa, respectively, while q is specific humidity, $\vec{V} = (u, v)$ is horizontal winds, and g is gravity. In the composite analysis, each variable can be written as the sum of three terms, e.g., $q = \overline{\overline{q}} + \overline{q}' + q'$, where q the is daily specific humidity, $\overline{\overline{q}}$ is the composite mean of monthly specific humidity, $\overline{q}'$ is the monthly departure from the composite mean, and q' is the daily departure from the monthly mean. The integrated part of transient moisture flux can be written as follows:

$$\overline{\overline{\vec{q'V'}}} = \overline{\overline{q\vec{V}}} - \overline{\overline{\vec{q}}}\,\overline{\overline{\vec{V}}} - \overline{\vec{q}}\,\overline{\vec{V}}, \tag{2}$$

where double overbar denotes averaging over 7 years within a composite, overbar denotes averaging over a month, prime denotes daily departure, and overbar-prime $\left(\overline{\ }'\right)$ denotes monthly departure. The composite

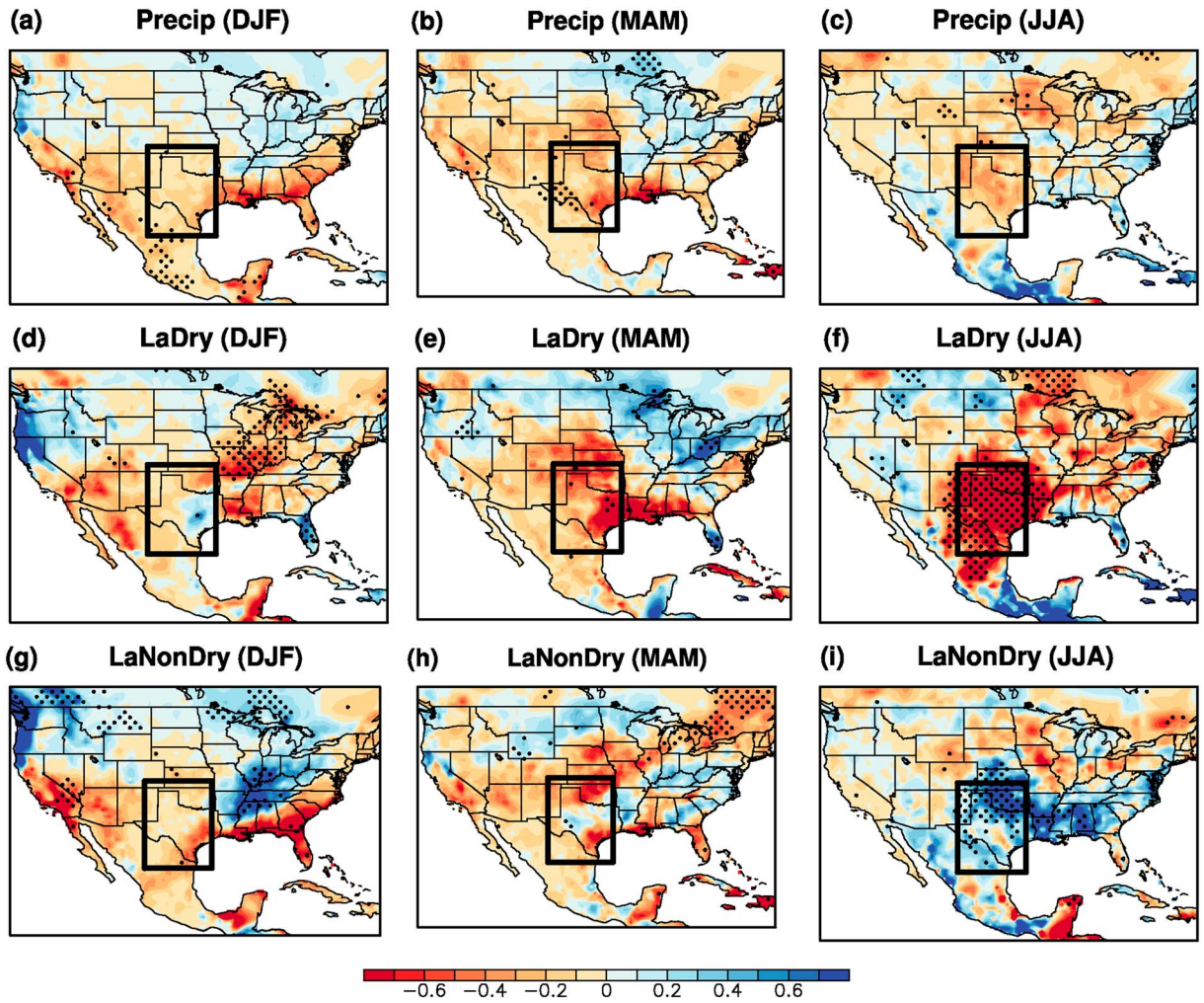

Figure 2. Precipitation anomaly (mm d^{-1}) composites of (a–c) 26 La Niña years, (d–f) LaDry, and (g–i) LaNonDry years. All figures show differences from climatological mean. Regions significant at the 90% confidence level (*t* test for Figures 2a–2c with reference to the climatology, bootstrap for Figures 2d–2i with reference to 26 La Niña years) are dotted. The black box denotes the SGP (95°–105°W, 25°–38°N).

total and mean flow (the first and second terms on the right-hand side of equation (2)) are shown in Figure 7. Moisture convergence is calculated in the same way.

3. Analysis

3.1. What Are the Anomalous Precipitation and Circulation Patterns Associated With Dry La Niña Years?

Figure 1a shows MJJA precipitation anomalies (turquoise and brown) over the SGP for La Niña years along with the CPC Niño 3.4 seasonal SSTA in JFMA (blue) and MJJA (red) in chronological order. Precipitation anomalies are defined relative to the 1971–2000 mean. Overall, more dry years (i.e., negative precipitation anomaly) than wet years occurred (16 versus 10) when there was La Niña. Among these 16 drier years, 11 years are associated with La Niña in JFMA while 10 years are associated with La Niña in MJJA, with five of these years associated with La Niña from JFMA to MJJA. As mentioned earlier, La Niña may occur at different time of a year. The seasonal dependence of SGP drought on La Niña and other factors will be discussed in detail in section 3.3. Anomalous dry conditions occurred in each decade from the 1950s to present, but fewer during the 1970s, indicating some decadal scale variations of precipitation during La Niña years.

Figure 1b shows the seasonal cycle of SGP precipitation (yellow bars) and the differences of precipitation (blue) and vertically integrated mass-weighted monthly moisture convergence (green) between La Niña

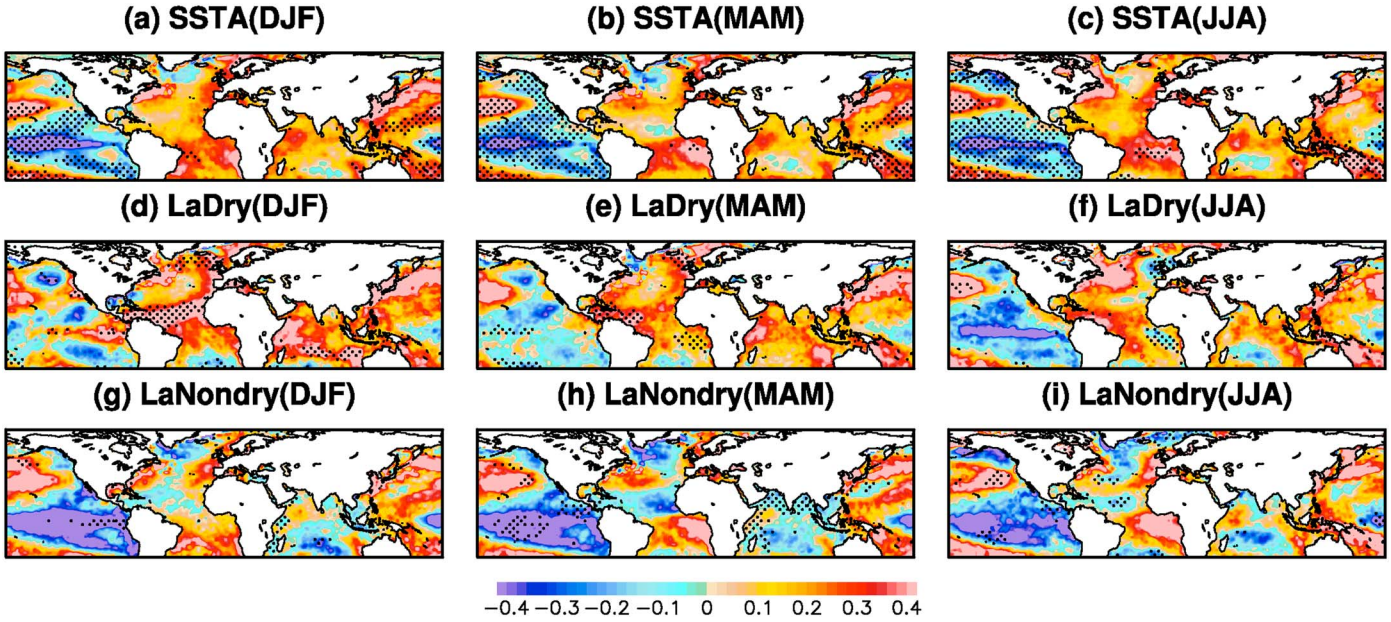

Figure 3. SSTA (K) composites of (a–c) 26 La Niña years, (d–f) LaDry, and (g–i) LaNonDry years. Regions significant at the 90% confidence level (*t* test for Figures 3a–3c with reference to the climatology, bootstrap for Figures 3d–3i, with reference to 26 La Niña years) are dotted.

dry and nondry years. The SGP precipitation generally peaks during May–September, with relatively low precipitation during July–August, associated with the "midsummer drought" over Mexico. The precipitation differences between the LaDry and LaNonDry composites also peak during MJJA, with the largest reduction of about 1.4 mm d^{-1} (~60%) in June. The decrease of vertically integrated moisture convergence is consistent with this precipitation reduction, but with its greatest reduction in May, about 1 month ahead of the maximum of precipitation reduction. From June to September, the reduction of moisture divergence is less than that of precipitation, indicating a contribution from reduced evapotranspiration (based on column moisture budget, precipitation is roughly equal to the sum of moisture convergence and evapotranspiration from the land surface) and possibly a contribution from eddy moisture divergence.

The LaDry and LaNonDry composites characterize conditions of the 27% driest and 27% wettest La Niña years over the SGP. To determine what causes their differences and how they relate to Niño 3.4 SST, we first examine the apparent effect of La Niña on precipitation and large-scale circulation patterns and then compare these relationships for all La Niña years with those for occurrence of dry anomalies. Figures 2a–2c shows the composite of precipitation anomalies (with reference to 1971–2000 mean) over the 26 La Niña years from DJF to JJA, while Figures 2d–2f and 2g–2i show the composites of precipitation anomalies for LaDry and LaNonDry years, respectively. The black box indicates the averaging area for SGP precipitation.

During winter, negative Niño 3.4 SSTs are related to negative precipitation anomalies along the southeast U.S., SGP, and southwest (Figure 2a), a pattern similar to that shown by *Seager et al.* [2009] and *Kushnir et al.* [2010]. These negative precipitation anomalies weaken over the southeast coast but extend into the northern plains in MAM (Figure 2b). During JJA, a significant dry anomaly is centered in the Northern Great Plains and a wet anomaly is located along the Gulf Coast and over Mexico (Figure 2c). In dry years, negative precipitation anomalies develop in the SGP in MAM and intensify in JJA (Figures 2e–2f). The spring precipitation anomaly pattern for dry years is similar to that of the all La Niña composite, but with a stronger magnitude over the eastern SGP, and in summer, dry years have a very significant dry anomaly pattern over the SGP, different from that of the all La Niña composite. Similarly, the wet anomalies in nondry years also set up in spring and strengthen in summer (Figures 2h and 2i).

Figure 3 displays the SST anomalies that correspond to the precipitation anomalies in Figure 2. Overall, the negative tropical Pacific SSTA in the composites for dry years (Figures 3d–3f) is weaker than that for the nondry years (Figures 3g–3i). In addition, in the dry composite, anomalous warming over the tropical North Atlantic persists from winter to spring, while in the nondry composite, anomalously cold tropical Atlantic

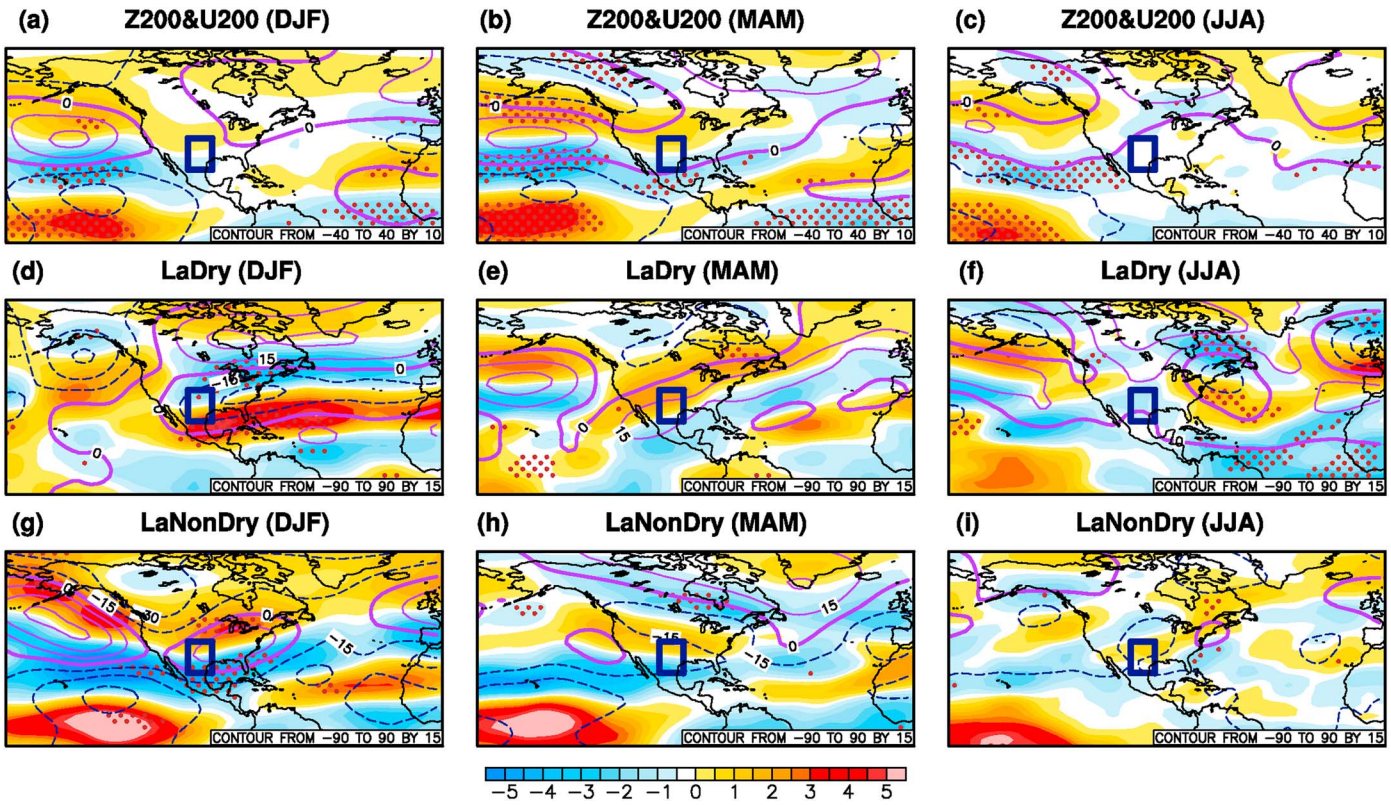

Figure 4. Composites of 200 hPa geopotential height (gpm; contours) and zonal wind (m s^{-1}; shading) anomalies in (a–c) 26 La Niña years, (d–f) LaDry, and (g–i) LaNonDry years. Areas with zonal wind anomalies significant at the 90% confidence level are dotted (*t* test for Figures 4a–4c with reference to the climatology, bootstrap for Figures 4d–4i with reference to 26 La Niña years). Contour interval is 15 gpm. Contours of zero (thick purple) and positive (negative) geopotential height anomalies are potted in purple (navy).

SSTA lasts from spring to summer. How the SST differences between the dry and nondry composites contribute to precipitation responses will be discussed in more detail in the following section.

Figures 4a–4c show anomalous 200 hPa geopotential heights (contours) and zonal winds (shading) in all La Niña years, consistent with the precipitation patterns and indicating wave patterns related to La Niña. In typical La Niña years, associated with the wave train developed from the tropical Pacific, a high anomaly is located over the northern North Pacific in winter and spring that extends to the southern U.S. in spring (Figures 4a and 4b). In summer, this high anomaly is shifted to the northern U.S., favoring dryness in the northern plains (Figure 4c). The 200 hPa zonal wind anomalies show the change of subtropical jet streams. La Niña has been related to a northward shift of the Pacific jet stream and storm tracks [e.g., *Trenberth et al.*, 1988; *Liu et al.*, 1998], as is seen in the all La Niña composite in DJF and MAM, but is weaker in JJA (Figures 4a–4c). Such a poleward shift of this jet stream can also affect the propagation of transient eddies and the eddy-driven mean meridional circulation and result in eddy-driven descent in the midlatitudes that suppress precipitation [*Seager et al.*, 2003, 2005a, 2005b].

The LaDry composite shows rather different anomalous circulation patterns from those of the all La Niña composite. In winter, an anomalous upper tropospheric low, instead of high, pressure center occurs over the northern Pacific (Figure 4d). A strong anomalous upper tropospheric low and equatorward shift of the jet stream also occur over the southern U.S. and middle latitude North Atlantic. In spring, the upper level anomalous low center shifts to the north-central North American continent (Figure 4e), instead of over the north-west North America and North Pacific as typically seen during La Niña years (Figure 4b). The jet stream over North America and the anomalous high over the SGP are also much stronger than those of a typical La Niña. In summer, the anomalous high over central North America dips down to the SGP (Figure 4f) and presumably contributes to a stronger dry anomaly over the SGP. A strong anomalous low, stronger than that in a typical La Niña summer, also appears over the eastern U.S.

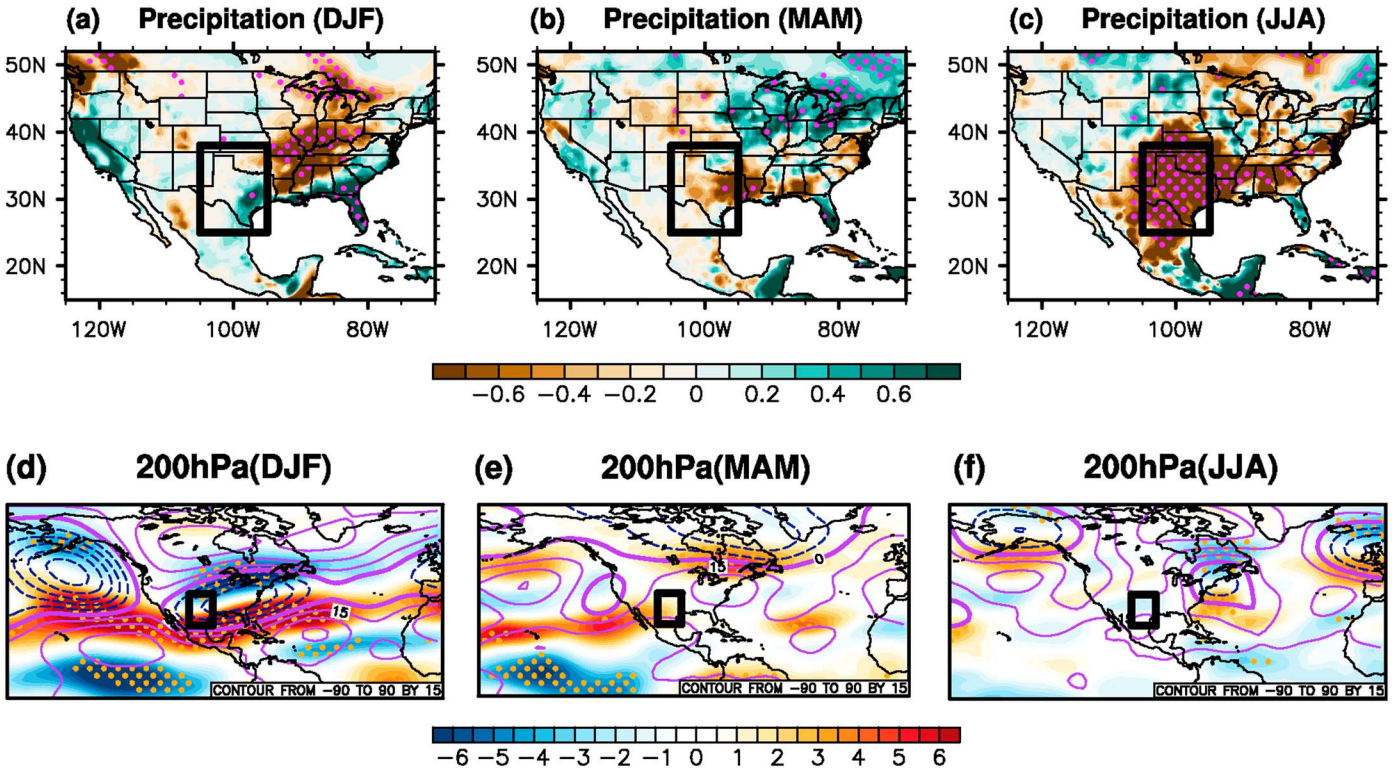

Figure 5. (a–b) Precipitation (mm d^{-1}) and (d–f) 200 hPa geopotential height (gpm; contours) and zonal wind (m s^{-1}; shading) differences between the LaDry and LaNonDry composites from DJF to JJA. Areas with precipitation and zonal wind anomalies significant at the 90% confidence level are dotted (Bootstrap). Contours of zero (thick purple) and positive (negative) geopotential height anomalies are plotted in purple (navy).

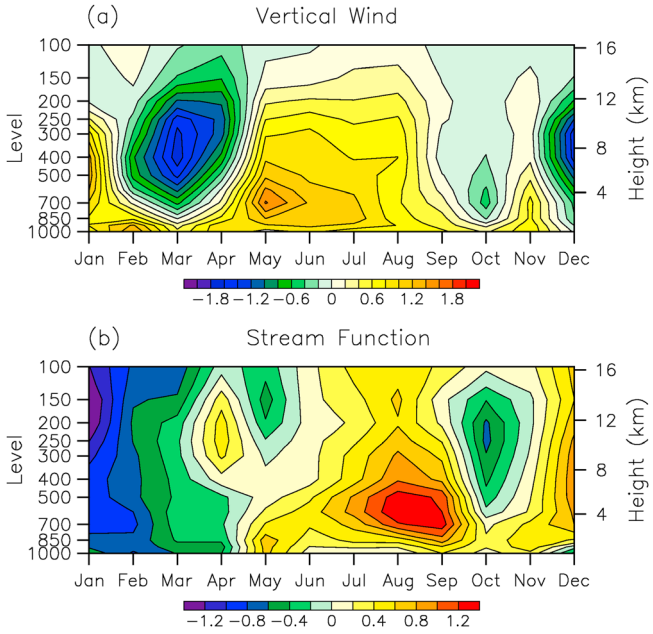

Figure 6. Time-pressure profile for the differences of (a) vertical velocity in pressure coordinates (10^{-2} Pa s^{-1}; positive anomalies denote downward motion and negative values denotes upward motion) and (b) standardized stream function averaged over the SGP between the LaDry and LaNonDry composites.

During the nondry years, the polarity of the north-south dipole of anomalous geopotential height over North America in winter and spring seasons is the opposite of that during LaDry years: An anomalous high dominates south-central and southeastern U.S. in winter and an anomalous low dominates southern U.S. in spring (Figures 4g and 4h), consistent with wetter conditions over that region. In summer, opposite to that of dry years, an anomalous low is centered over the SGP (Figure 4i), favoring precipitation.

To show more clearly the contrast between the LaDry and LaNonDry conditions, we evaluate their differences in Figures 5–8. Figure 5 shows these differences in precipitation and circulation anomalies. The precipitation anomalies in Figures 5a–5c resemble those of dry years (Figures 2d–2f) but with greater magnitudes. In DJF, there is little precipitation difference over the SGP, but a large deficit in the Mississippi river basin (Figure 5a), somewhat opposite to that

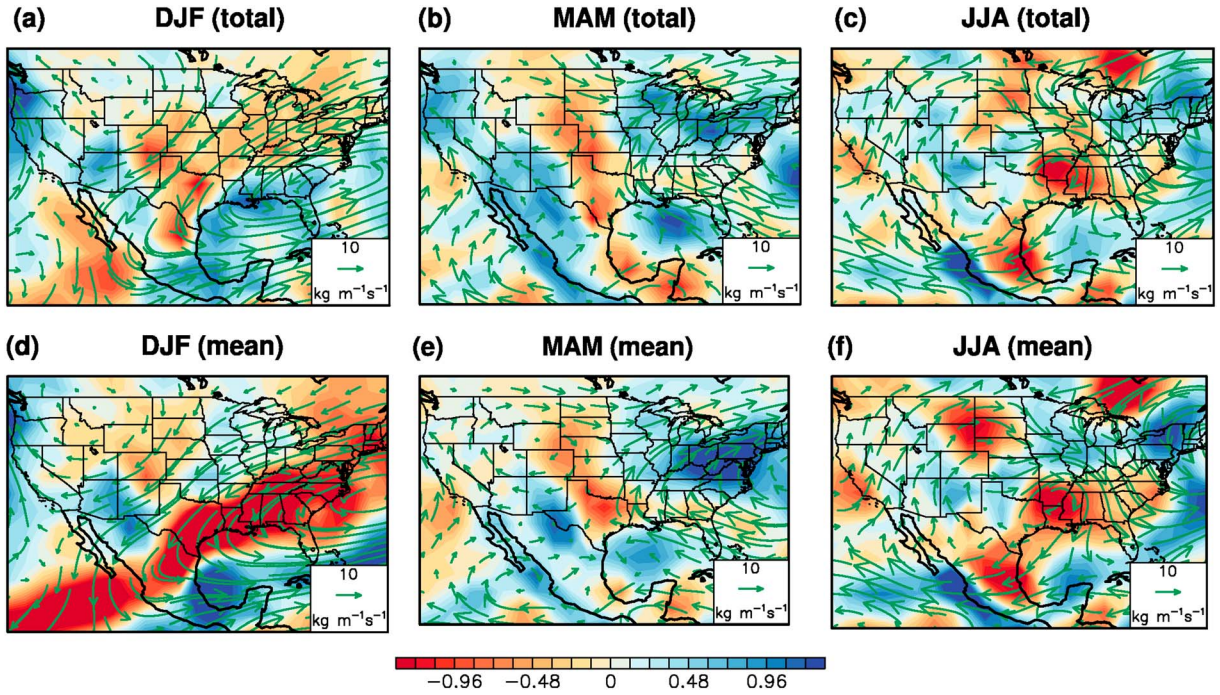

Figure 7. Anomalies of vertically integrated (from surface hPa to 300 hPa) mass weighted moisture transport (vectors; kg m^{-1} s^{-1}) and moisture convergence (mm d^{-1}; shading, positive value for convergence) for the differences between the LaDry and LaNonDry composites from DJF to JJA. (a–c) total, (d–f) mean flow moisture fluxes (from equation (2)), and convergence. Total moisture convergence/flux is calculated from daily NCEP1 reanalysis, mean flow convergence/flux uses monthly mean values (see section 2.6 for details).

of all La Niña years (Figure 2a). The pattern in MAM is similar to that of Figure 2b, i.e., dryness along the Gulf Coast from its eastern edge into the SGP (Figure 5b). JJA shows a large deficit centered over the SGP, southeast U.S., and northern Mexico (Figure 5c). The differences of geopotential heights between dry and nondry years (Figures 5d–5f) also resemble those of the dry composite (Figures 4d–4f), showing patterns that somewhat resemble those of typical La Niña years over the U.S. in MAM, but nearly opposite in DJF and also quite different in JJA. In MAM, an anomalous high is located over most of the U.S. with a center over the East Coast and an anomalous low over the West Coast (Figure 5e). In JJA, an anomalous high is centered over northern Canada and extends to the western U.S. and SGP with a low centered over the eastern U.S. (Figure 5f), favoring the dryness. Also, differing from typical La Niña years, geopotential heights are anomalously positive over the tropical North Atlantic from winter to summer, suggesting an influence from the North Atlantic. The North Pacific and Atlantic jet streams are shifted southward in DJF but displaced northward during MAM, and again southward in the North Atlantic during JJA (Figures 5d–5f), displacing the storm track away from the SGP and thus supporting the development and intensification of the dry anomaly.

Anomalously high geopotential heights are usually associated with subsidence. Figure 6 shows the differences of downward vertical velocity in pressure coordinates (ω) and stream function averaged over the SGP box between the LaDry and LaNonDry composites. Figure 6a shows that stronger subsidence from the surface to upper levels occurs from March to September, consistent with reduced precipitation in this period. Figure 6b shows a high pressure anomaly develops from May to October with initially an almost barotropic structure. This high pressure peaks later than the vertical motion (in JAS versus MJJ), presumably a result of positive feedbacks from lower troposphere and near surface, e.g., a reduction of soil moisture that amplifies the dryness [e.g., *Fernando et al.*, 2015; D. N. Fernando et al., submitted to *Climate Dynamics*, 2015].

Figure 7 shows differences of total and mean flow moisture fluxes (vectors) and moisture convergence (shading) between the two composites from DJF to JJA. The contribution from transient moisture convergence weakens mean flow divergence in winter but is relatively small in spring and summer as can be inferred from the pattern resemblance of Figures 7b and 7c versus 7e and 7f. Anomalous total moisture divergence is seen over the SGP from DJF to MAM (Figures 7a and 7b) but shifted to the central Gulf Coast in JJA (Figure 7c),

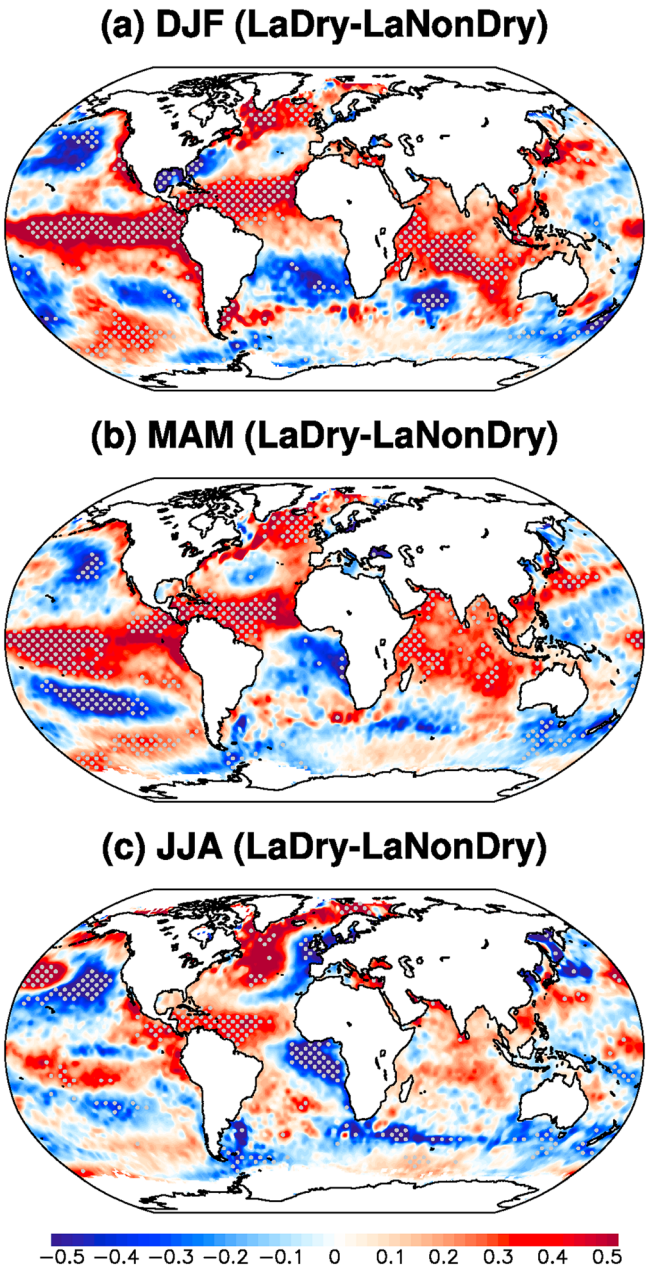

Figure 8. Differences of SST (K) between the LaDry and LaNonDry composites. Areas significant at the 90% confidence level are dotted (bootstrap).

while anomalous moisture convergence is located over the southeast coast in DJF, Midwest in MAM, and the northeast in JJA. These anomalies of total moisture convergence agree with precipitation anomalies (Figures 5a–5c) but with some differences. A discrepancy between observed precipitation and NCEP1 moisture convergence is also noted by *Seager et al.* [2014]. The pattern of anomalous mean flow moisture flux (Figures 7d–7f) generally resembles that of the total moisture flux but shows different gradients as revealed by moisture convergence anomalies. Much stronger mean flow moisture divergence occurs over the SGP and the Gulf Coast in DJF (Figure 7d), which is mainly balanced by the anomalous transient moisture convergence as can be inferred from the weaker reversed value seen in Figure 7a. In spring, mean flow moisture divergence is located over northeastern Texas, while a strong anomalous convergence is located over the northeastern U.S. (Figure 7e). In summer, mean flow moisture divergence to the east of the SGP (Figure 7f) is stronger than that from total moisture divergence (Figure 7c), while weak convergence occurs to the northwest of the SGP, perhaps due to shallow cyclonic circulation anomalies driven by surface heating. In short, mean flow dominates the total moisture convergence and flux in spring and summer. Transient moisture flux is only important for weakening the mean flow moisture divergence in DJF but has a relatively weak such effect in other seasons.

To summarize, Figures 5–7 show that a decrease of precipitation from nondry to dry La Niña years in MAM is associated with a northward shift of the subtropical jet stream and anomalous high and subsidence over the SGP that inhibit the convection. Local geopotential height gradients are modified to reduce the moisture flux and convergence to the SGP. We now investigate what SSTA patterns may be sources of these circulation anomalies between dry and nondry years.

3.2. Anomalous SST Patterns Associated With La Niña Dry and Nondry Years

Figure 8 shows the differences of SST between the LaDry and LaNonDry composites from DJF to JJA. These SSTA pattern differences in the Pacific are mainly a consequence of the strong La Niña SSTAs that occur during nondry La Niña years. The main differences in the Atlantic is an anomalously high SST over the tropical and middle- to high-latitude North Atlantic Ocean, i.e., a pattern somewhat similar to a positive AMO pattern but on an interannual time scale. This pattern persists from winter to summer but with a weaker magnitude in

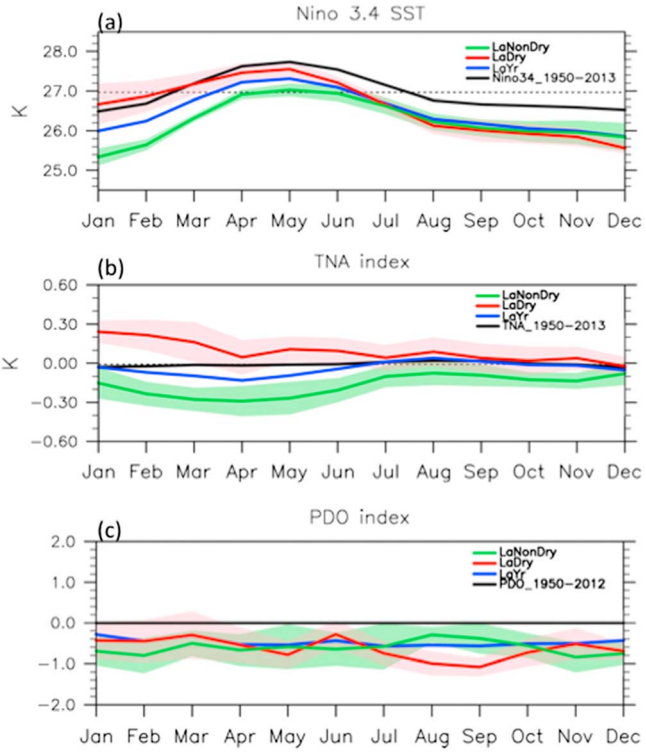

Figure 9. Seasonal cycle of three oceanic indices in their climatological means (black lines), averages over the 26 La Niña years (blue) and the LaDry (red) and LaNonDry (green) composites. Shading shows ±1 standard error. (a) Niño 3.4 SST and (c) PDO indices are from the CPC. (b) The TNA index is calculated from HadISST.

summer. The SST over the Gulf of Mexico and along the southeast coast in DJF is lower for dry years but not in other seasons, possibly contributing to the anomalous northerly flow from land to the Gulf at that time by reinforcing the anomalous high at lower latitudes over the southern Gulf (Figure 5d). The South Atlantic SST differences also decrease from DJF to JJA, indicating a northward shift of the Atlantic Intertropical Convergence Zone.

Figure 8 shows a pattern of tropical Pacific SSTs that is less La Niña like in dry years than in nondry years but mainly in DJF and MAM. This difference over the Pacific would be smaller if 1998, which was El Niño from winter to spring but switched to La Niña in the summer, were removed from the LaDry composite. The anomalous circulation patterns between the LaDry and LaNonDry composites would not otherwise change much. An anomalous cold SST over the midlatitude North Pacific occurs in DJF (Figure 8a), resembling a positive PDO pattern, but this SSTA switched to a pattern resembling that of negative PDO pattern in JJA (i.e., as indicated by the red region in the North Pacific and the surrounding blue shading in Figure 8c).

An anomalous warming is also found over the Indian Ocean in winter (Figure 8) but weakens in spring and summer (Figures 8b and 8c). The role of Indian Ocean SST on U.S. drought is inconclusive according to previous studies. While warmer than usual Indian Ocean was found to contribute to the 1998–2002 U.S. continental-wide drought [e.g., *Hoerling and Kumar*, 2003; *Lau et al.*, 2006], *Seager* [2007] found that the Indian Ocean was anomalously cold in the previous five multiple-year droughts in the United States. Here we mainly focus on the contributions from the Pacific and Atlantic Oceans.

To further compare the SSTAs between dry and nondry La Niña years, seasonal cycles of Niño 3.4, tropical North Atlantic and PDO indices in the LaDry (red) and LaNonDry (green) composites are displayed in Figure 9, along with their climatological mean (black) and averages over 26 La Niña years (blue). Figure 9a shows that the climatological Niño 3.4 SST is relatively warm from March to July, with a peak in May. A similar seasonal cycle occurs in La Niña years but with cooler SST. Another interesting feature is the weaker La Niña SST anomalies in dry years than in nondry years from January to June. The differences of Niño 3.4 SSTA between the dry and nondry composites are indistinguishable in the latter half of the year.

Figure 9b shows the TNA index for La Niña years and the dry and nondry composites as anomalies with reference to the seasonal cycle to better reveal the differences between dry and nondry years. The tropical Atlantic SST index is also warmer in dry years than nondry years, and the differences are greater during late winter to summer. Previous studies [e.g., *Curtis and Hastenrath*, 1995; *Enfield and Mayer*, 1997; *Alexander et al.*, 2002] pointed out that winter La Niña may lead to cold SSTA in the tropical Atlantic in spring and summer. In winter, Niño 3.4 SSTAs in nondry years are colder than those in dry years, possibly resulting in colder tropical North Atlantic SSTA in spring and summer in nondry years (Figures 3h and 3i) and favoring wet conditions in the SGP.

In La Niña years, the PDO index is negative on average (blue line, Figure 9c), consistent with the pan-Pacific SST pattern found in previous analyses [e.g., *Schubert et al.*, 2009]. However, there is no significant

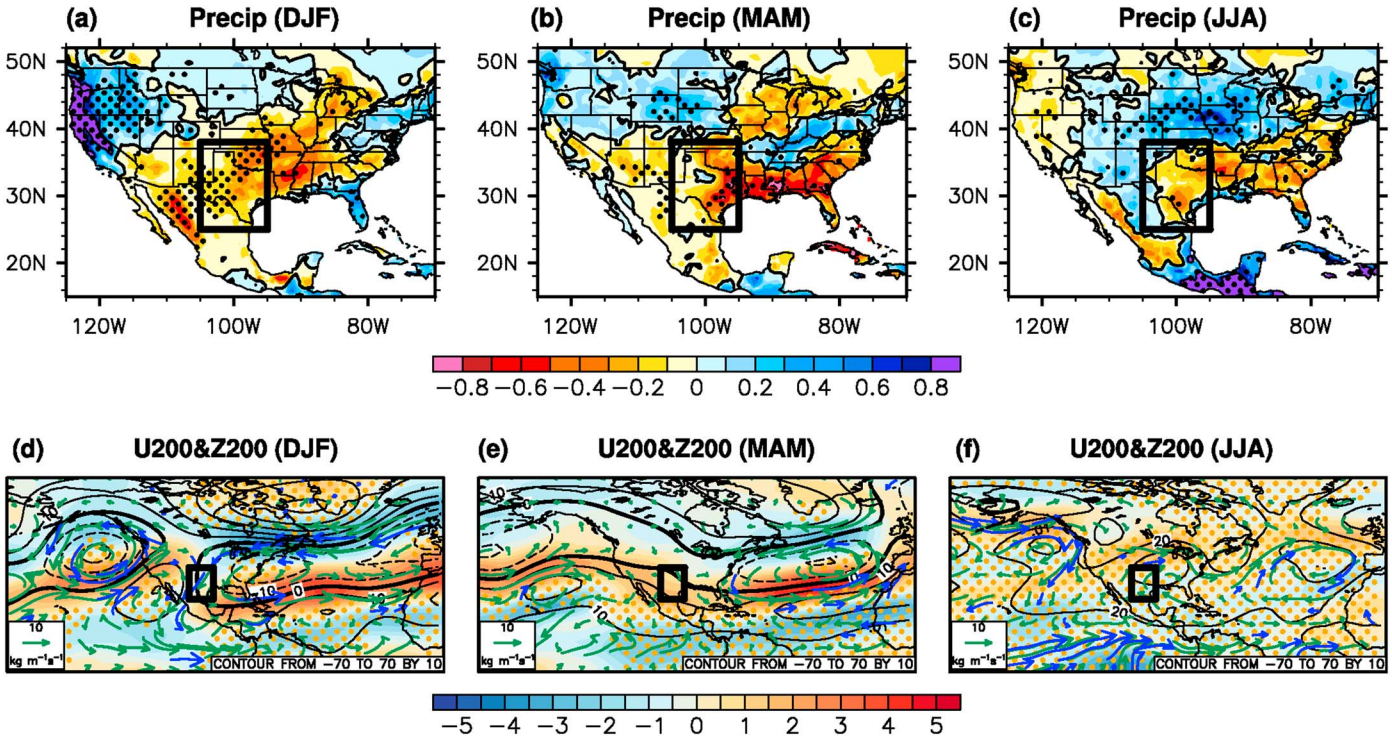

Figure 10. The TNA component of regressions of (a–c) precipitation (mm d^{-1}), (d–f) 200 hPa geopotential height (gpm; contours) zonal wind speed (m s^{-1}; shading), and vertically integrated mass weighted monthly moisture flux (vector; kg m^{-1} s^{-1}, vectors significant at the 90% confidence level are plotted in blue) onto the standardized TNA and Niño 3.4 indices during 26 La Niña years. Areas with precipitation and zonal wind anomalies significant at the 90% confidence level are dotted (*t* test).

difference in the magnitude of the PDO between the LaDry and LaNonDry years except during the August–September period.

How seasonal precipitation in the SGP in general relates to the tropical North Atlantic SST during La Niña years is examined through teleconnection patterns. Multiple linear regressions using the TNA and Niño3.4 indices are applied to precipitation, 200 hPa geopotential height, and zonal wind fields. The regression patterns in Figure 10 show how these variables are associated with variations of the TNA index when the Niño 3.4 index is held constant. A positive SSTA is accompanied by a reduction of precipitation in the SGP from winter to summer (Figures 10a–10c). Anomalously warm tropical North Atlantic SSTs are associated with an anomalous low at 200 hPa over the middle North Atlantic and eastern U.S., and weaker southerly moisture transport and stronger divergence over the SGP in spring (Figure 10e) and winter (Figure 10d). In summer, the North Atlantic and the U.S. are influenced by anomalous highs associated with the warmer tropical North Atlantic, and the jet stream shifts northward (Figure 10f).

3.3. Relative Influences of SSTs Versus the NAO

Figures 8 and 9 suggest that the different precipitation response to La Niña between dry and nondry years is related to both tropical North Atlantic and tropical Pacific SSTs. Which is more important on an interannual scale? What is the role of atmospheric internal variability such as that of the NAO in determining the dry or nondry La Niña years? Figure 11 shows the regression coefficients (in absolute values) of SGP precipitation onto the SST-based indices and the NAO index during 26 La Niña years. Among the four indices, Niño 3.4 SST is most important over a large portion of the domain in DJF (Figure 11a), while the tropical North Atlantic SST dominates the precipitation anomalies over northeastern SGP and northwestern Mexico during MAM (Figure 11b). The NAO has significant influence over central Texas in spring and dominates the SGP precipitation anomalies in JJA (Figures 11b and 11c). The influences of the Atlantic in spring and of the NAO on U.S. Great Plains precipitation have been reported previously, for example, by *Nigam et al.* [2011] on the decadal scale. The influences of the NAO on the Great Plains low-level jet in summer have also been

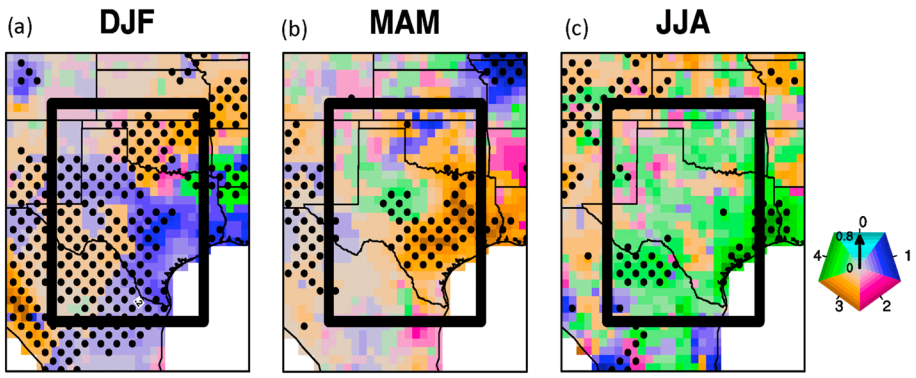

Figure 11. Multiple linear regression coefficients of precipitation onto the standardized 1-Niño 3.4, 2-PDO, 3-TNA, and 4-NAO indices for 26 La Niña years during (a) DJF, (b) MAM, and (c) JJA. Regression coefficients significant at the 90% confidence level (*t* test) are dotted. Color denotes the index that contributes most to precipitation among the four indices (i.e., largest coefficient in absolute value). Blue, maroon, brown, and green denote the Niño 3.4, PDO, TNA, and NAO indices, respectively. Saturation of the colors shows the magnitude of the coefficient (0 to 0.8).

reported [*Ruiz-Barradas and Nigam*, 2005; *Weaver and Nigam*, 2008]. However, their relative roles in determining the occurrence of summer drought over the SGP during La Niña years have not been previously investigated. Figure 11 suggests that tropical North Atlantic SSTA in spring and the NAO in summer could work in concert with a La Niña effect on winter soil moisture to increase the risk of summer drought over the SGP.

Table 2 shows the percentage of total variance of SGP precipitation that can be explained by the Niño 3.4, PDO, TNA, and NAO indices during La Niña years and all years, respectively. These four indices together explain about 37% of the total precipitation variance in La Niña winters, 26% in spring, and about 18% in summer. Table 2 also indicates that in La Niña years more than 50% of the precipitation variance during winter to summer cannot be explained by the above factors and may be related to random atmospheric variability, land-atmosphere feedbacks, and other remote forcing that have not been examined here, e.g., influences from the Indian Ocean. Precipitation variance in those La Niña years with relatively large precipitation anomalies, i.e., the seven driest years and seven wettest years (Table 1), are better explained by these factors, especially in winter and summer (Table 2). This better explanation suggests that strong SSTAs and NAO may be important for the development of severe droughts and floods but less so for weaker events.

How does the NAO relate to dry and nondry La Niña years? Figure 12a shows that the NAO index does not show a significant difference between the LaDry and LaNonDry years except for July–September, with a negative NAO index associated with LaDry years. During MAM, although positive NAO appears to contribute to four out of seven LaDry years, the composite NAO difference between LaDry and LaNonDry is insignificant because of large variation of NAO phases among the LaDry years. Teleconnections between the NAO index and precipitation, 200 hPa zonal wind speed, and geopotential height in MAM and JJA are shown in Figures 12b–12e. In spring a positive NAO is associated with reduced precipitation over the northern plains, western U.S., and central Texas (consistent with Figure 11b) and increased precipitation over the northeastern U.S. Such a precipitation anomaly pattern is consistent with 200 hPa geopotential height and zonal wind anomalies (Figure 12d), i.e., an anomalous high is colocated with a dry anomaly over the U.S., along with a northward shift of the jet stream over the Atlantic. However, in JJA an anomalous negative NAO is associated with reduced precipitation over the SGP and southeastern U.S. (Figure 12c), shifting the 200 hPa jet stream northward and increasing 200 hPa geopotential height over the SGP (Figure 12e), both favoring drought development in summer. Along with these circulation changes, moisture

Table 2. The Total Variances of SGP Precipitation Explained (%) by the Niño3.4, PDO, TNA, and NAO Indices Using Partial Least Squares Regression (First Three Components) for All the Years During 1950–2012 and for 26 La Niña Years[a]

	La Niña Years	1950–2012
DJF	36.6 (54.7)	33.8
MAM	25.5 (26.1)	17.4
JJA	17.5 (45.5)	8.1

[a]Variances explained in the 14 LaDry and LaNonDry years are shown in brackets.

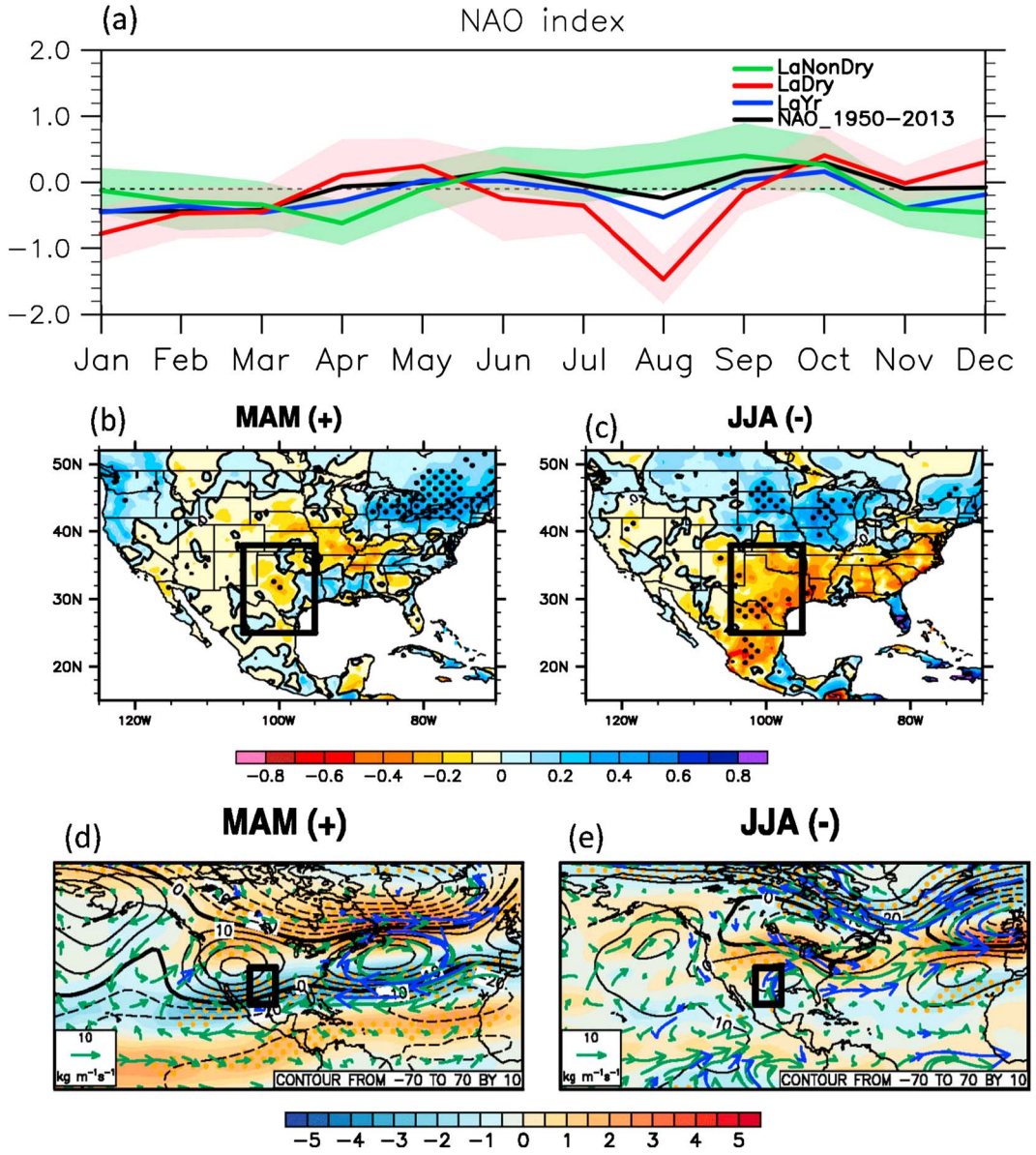

Figure 12. (a) Seasonal cycle of the NAO indices for its climatological mean (1950–2013 average; black lines), an average over 26 La Niña years (blue), and the LaDry (red) and LaNonDry (green) composites. Shading shows ±1 standard error. Regressions of precipitation (mm d^{-1}) in (b) MAM and (c) JJA, and regressions of 200 hPa zonal wind (m s^{-1}; shading) geopotential height (gpm; contours) and vertically integrated mass-weighted monthly moisture flux (vector; kg $m^{-1}s^{-1}$, vectors significant at the 90% confidence level are plotted in blue) in (d) MAM and (e) JJA onto the standardized NAO index (multiplied by −1 for JJA) during 26 La Niña years. Areas with precipitation and zonal wind anomalies significant at the 90% confidence level are dotted (*t* test).

fluxes are also modified to favor summer drought in the SGP, i.e., enhanced southerly flow from the Gulf to the northern plains, resulting in moisture divergence over the SGP.

To what extent can the anomalous circulation pattern be explained by the SSTA and NAO indices? Figure 13 shows reconstructed (see figure caption for details) 200 hPa geopotential height using different linear combinations of the indices discussed above for the differences between the LaDry and LaNonDry composites. Figures 13a–13c show the circulation patterns linearly associated with the Pacific SSTAs (i.e., reconstructed height field using the Niño 3.4 and PDO indices). Figures 13d–13f show the anomalous height associated with the four indices. The similarities of the spatial pattern between the reconstructed height field (e.g., Figures 13d–13f) and

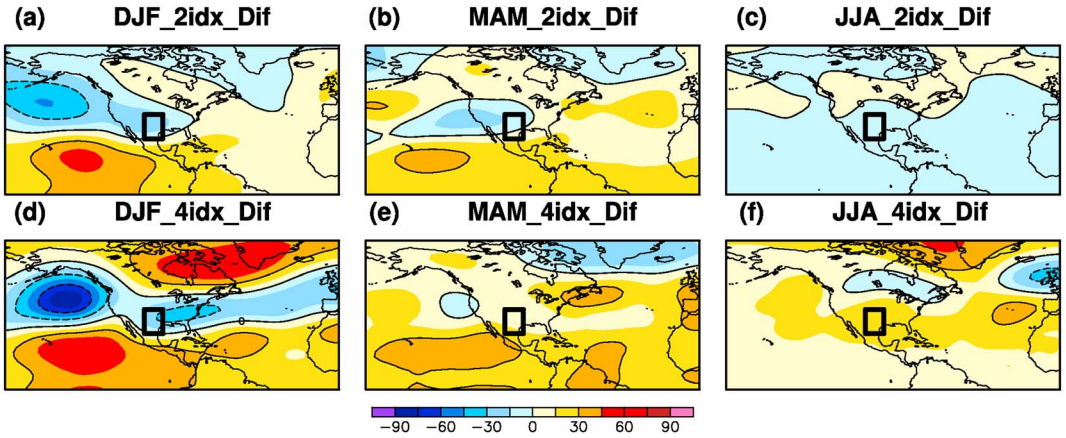

Figure 13. Reconstructed 200 hPa geopotential height differences (gpm) between the LaDry and LaNonDry composites using (a–c) PDO and Niño3.4 indices, and (d–f) four indices during 26 La Niña years from DJF to JJA. Take Figure 13a, for example, first, the multiple linear regression coefficients were obtained by regressing the 700 hPa geopotential heights onto standardized Niño 3.4, PDO, TNA, and NAO indices during the La Niña years. Then the reconstructed height fields for the LaDry and LaNonDry composites were obtained by multiplying the Niño 3.4 and PDO indices averaged over the seven dry and seven nondry years with the corresponding regression coefficients, respectively. Finally, the differences of reconstructed height between the LaDry and LaNonDry composites were calculated. Shading interval is 15 gpm, while black contour interval is 30 gpm.

that in the NCEP1 (Figures 5d–5f) suggest that some large-scale circulation features are associated with the above mentioned indices.

Including the TNA and NAO indices amplifies the geopotential height anomalies in winter (Figure 13d) and places the anomalous high center to northeastern U.S. in MAM (Figure 13e), which is more similar to that for the differences between LaDry and LaNonDry years in the NCEP1 (Figure 5e) than obtained only using the Pacific indices (Figure 13b). In summer, the anomalous high over the southwestern U.S. and the SGP is captured to some extent. The anomalous high centers in the northern North America and Atlantic and over northern North Pacific are also captured (Figure 13f). Table 3 shows pattern correlations (centered) between the reconstructed geopotential height fields and those for the differences between LaDry and LaNonDry years. The height field in MAM and JJA is best represented when using the four indices. This best agreement suggests that a large portion of circulation differences between the dry and nondry years are contributed by the differences of the NAO and tropical North Atlantic SSTA in these years.

Figure 14 shows reconstructed precipitation for differences between the LaDry and LaNonDry composites using the four indices and the percentage of SGP precipitation anomalies that is reconstructed using different combination of the indices during MAM and JJA, when the dry anomaly is established and intensified. The patterns of reconstructed precipitation anomaly (Figures 14a and 14b) resemble closely those observed (Figures 5b and 5c), but their magnitude is only about one half. In JJA, the dry anomaly is located closer to the Gulf Coast while the wet anomaly is located farther east. Averaged over the SGP domain (Figure 14c), the precipitation differences (i.e., LaDry minus LaNonDry) associated with Pacific SSTA (Niño 3.4 and PDO) are opposite in sign from that observed in spring (light purple). The TNA and NAO indices together contribute 63% of the precipitation differences over the SGP between the dry and nondry composites, with a roughly equal contribution from the tropical North Atlantic and NAO (33% and 30%, respectively). In summer (purple), precipitation differences cannot be reconstructed by the three SSTA indices and only the NAO appears to have some influence, contributing to about 20% of the total precipitation

Table 3. Pattern Correlation (Centered) Between NCEP1 200 hPa Geopotential Height (Figures 5d–5f) and the Reconstructed Geopotential Height (Figure 13) Over the North Pacific-North America-North Atlantic Region (5°S–75°N, 0°–180°W) Using Different Indices (Niño3.4, PDO, TNA, and NAO) for the Differences Between the LaDry and LaNonDry Composites

	Niño3.4 + PDO	Niño3.4 + PDO + TNA + NAO
DJF	0.80	0.96
MAM	0.69	0.70
JJA	−0.12	0.73

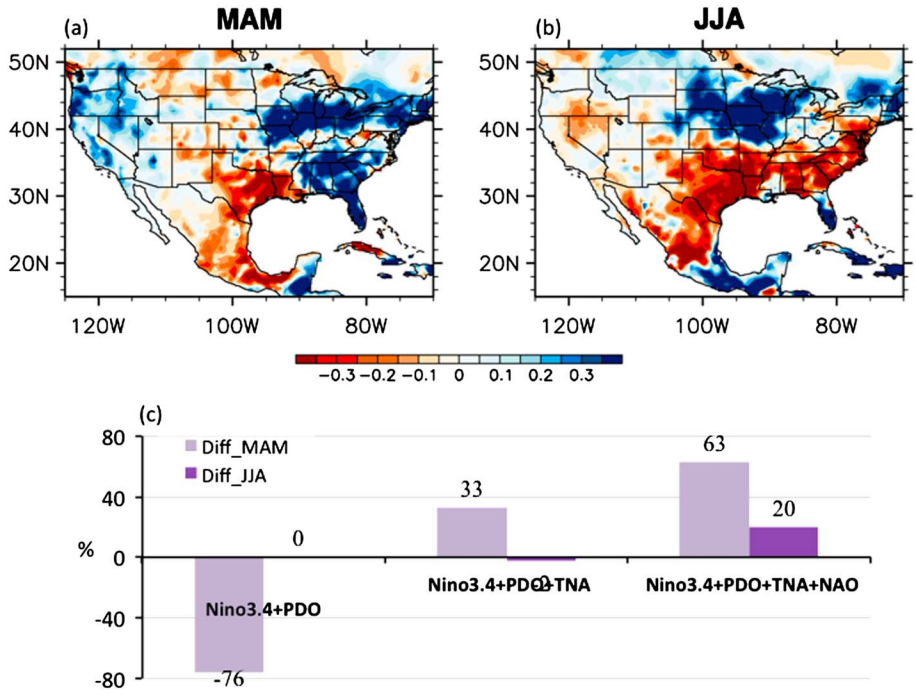

Figure 14. Reconstructed precipitation differences (mm d^{-1}) between the LaDry and LaNonDry composites using four indices (Niño 3.4, PDO, TNA, and NAO) for (a) MAM and (b) JJA, and (c) percentage of SGP precipitation anomalies can be reconstructed by the different combination of indices (through multiple linear regressions, the same method as in Figure 13 but for precipitation) in MAM (light purple) and JJA (purple). Negative values indicate that the sign of reconstructed precipitation anomalies is opposite to observation.

differences. Thus, Figure 14c also indicates that in summer internal variability, such as the NAO, has a stronger influence on precipitation anomalies than the three SSTA indices, consistent with Figure 11c.

4. Discussion

La Niña has long been related to precipitation deficits in the SGP. This paper examines 26 La Niña events from 1950 to 2013 to understand the differences in circulation and SST anomaly patterns accompanying dry versus nondry summer in the SGP. The dry summers over the SGP starts to establish in MAM, along with the development of anomalous high geopotential height and subsidence. Their geopotential height gradients and consequently wind and moisture fluxes show enhanced mean flow moisture flux and moisture convergence into the northern plains and Midwest and reduced over the SGP. Transient moisture convergence in the SGP has an opposite sign from that of the mean flow moisture divergence but is substantially weaker in spring and summer. At 200 hPa, the subtropical jet streams are shifted northward, favoring drought development. With these favorable atmospheric conditions, a negative precipitation anomaly is maintained and intensified from spring to summer, leading to strong summer droughts.

We examine what SST anomalies may be related to these anomalous circulation patterns. One dominant feature is the anomalous warming of the tropical North Atlantic. This SST anomaly is accompanied by an increase of the geopotential height over the northern and tropical Atlantic, Gulf of Mexico, the southwestern and northern U.S., but a reduction over the subtropical western Atlantic. Thus, the anomalous high centered over the SGP is strengthened. In the upper troposphere, the jet streams are also weakened over the SGP in winter and spring. Another feature is weaker La Niña-like SST anomalies in dry years than in nondry years. Such a weaker La Niña perhaps allows warmer tropical North Atlantic SST to modify circulation and thus favors the development of drought in the SGP in MAM. On the other hand, the stronger winter La Niña in the nondry years combined with cold SSTA in the tropical North Atlantic in spring promotes wet conditions in the SGP. A weakly positive anomalous PDO pattern is also found in DJF but switches to negative in JJA.

The NAO has been previously related to SGP drought development in winter [e.g., *Seager et al.*, 2014]. Our analysis shows that the NAO index in the summer of dry years is more negative than in nondry years. The geopotential height in the SGP is correspondingly enhanced with this anomalous negative NAO, along with a poleward displacement of the North Atlantic jet stream, both of which tend to reduce SGP precipitation. In spring, a positive NAO may also reduce precipitation over north central Texas, although the differences of the NAO between the dry and nondry years are not significant in MAM.

The anomalous precipitation, circulation, and SST patterns discussed above are also consistent with those composites for all dry SGP years (not shown), suggesting that they are robust in representing the characteristics of anomalous circulation, SSTA, and atmospheric internal variability associated with a dry SGP. In individual dry years, one or several of these factors combined to trigger or maintain the drought. For instance, the 2011 drought is associated with all of the above factors, i.e., a La Niña and a negative PDO in winter, warmer than usual tropical North Atlantic SSTA in spring, and a negative phase of the NAO in summer. In the 1956 drought, cold Pacific SSTAs occurred in winter favoring the drought development. Although in spring the tropical North Atlantic was slightly colder than usual, in summer the NAO anomaly was negative and again favored drought.

During 26 La Niña years, the above factors together may explain about 26% of SGP precipitation variances in spring and 18% in summer. The large (more than 50%) unexplained variance indicates a substantial amount of contribution from some combination of random atmospheric variability, nonlinear interactions among these factors, and nonlinear components of those positive feedbacks such as those involving land-atmosphere interactions.

However, in the years with relatively large precipitation anomalies (i.e., the 14 dry and nondry La Niña years listed in Table 1), up to 55% and 46% of precipitation variances can be explained by these indices in DJF and JJA, respectively, suggesting that large-scale SSTA and circulation anomalies play important roles in severe drought/flood development. This point is also supported by an examination of the differences of the SST and circulation patterns between SGP dry and nondry years (not shown).

5. Conclusions

Droughts (i.e., strong negative seasonal precipitation anomalies) in the Southern Great Plains (SGP) tend to occur in La Niña years, but La Niña alone does not necessarily lead to summer droughts. We look at what distinguishes the La Niña years driest summers in the SGP from those with least dry summers by looking at their pattern differences in circulation and precipitation and by examining tropical North Atlantic SST, PDO, and NAO patterns. Our analysis indicates that the previously recognized dependence of SGP drought on La Niña is only significant in winter.

The dependence of SGP drought on other contributing factors is seasonal. In particular, warm tropical North Atlantic SST can contribute to droughts over the southeastern SGP in spring. A negative NAO circulation anomaly becomes the only significant factor in summer during La Niña years.

Thus, the occurrence of strong drought in the SGP during the summer of La Niña years is contributed by a combination of SST anomalies and atmospheric internal variabilities that randomly reinforce each other. In particular, decrease of precipitation by La Niña and resultant drier soil moisture in winter followed by a warmer tropical North Atlantic SST in spring and a negative NAO index in summer are found to maximize the summer drought in the SGP. In individual drought years, one or several of these factors combined together to result in favorable conditions for drought development.

Acknowledgments

This work is supported by the NOAA Modeling, Analysis, Predictions, and Projections Program, the NASA Development and Testing of Potential Indicators for the National Climate Assessment Program (NNX13AN39G), and Climate Program Office Climate Prediction Program for the Americas (CPPA) grant (NA10OAR4310157). The Niño3.4 index was downloaded from http://www.cpc.ncep.noaa.gov/products/analysis_monitoring/ensostuff/ensoyears.shtml. Other CPC indices were from http://www.esrl.noaa.gov/psd/data/climateindices/list/. CRU TS 3.21 precipitation was downloaded from http://badc.nerc.ac.uk/view/badc.nerc.ac.uk__ATOM__ACTIVITY_0c08abfc-f2d5-11e2-a948-00163e251233. The NCEP/NCAR reanalysis product was obtained from http://www.esrl.noaa.gov/psd/data/reanalysis/reanalysis.shtml and HadISST from http://www.metoffice.gov.uk/hadobs/hadisst/data/download.html. Authors would like to thank the editor and three anonymous reviewers for their valuable comments.

References

Abudu, S., C. L. Cui, J. P. King, J. Moreno, and A. S. Bawazir (2011), Modeling of daily pan evaporation using partial least squares regression, *Sci. China Technol. Sci.*, *54*(1), 163–174, doi:10.1007/s11431-010-4205-z.

Alexander, M. A., I. Blade, M. Newman, J. R. Lanzante, N. C. Lau, and J. D. Scott (2002), The atmospheric bridge: The influence of ENSO teleconnections on air-sea interaction over the global oceans, *J. Clim.*, *15*(16), 2205–2231, doi:10.1175/1520-0442(2002)015<2205:Tabtio>2.0.Co;2.

Curtis, S., and S. Hastenrath (1995), Forcing of anomalous sea-surface temperature evolution in the tropical Atlantic during Pacific warm events, *J. Geophys. Res.*, *100*(C8), 15,835–15,847, doi:10.1029/95JC01502.

Dai, A., K. E. Trenberth, and T. R. Karl (1998), Global variations in droughts and wet spells: 1900–1995, *Geophys. Res. Lett.*, *25*(17), 3367–3370, doi:10.1029/98GL52511.

Enfield, D. B., and D. A. Mayer (1997), Tropical Atlantic sea surface temperature variability and its relation to El Niño Southern Oscillation, *J. Geophys. Res.*, *102*(C1), 929–945, doi:10.1029/96JC03296.

Fernando, D. N., R. Fu, R. S. Solis, R. E. Mace, Y. Sun, B. Yan, and B. Pu (2015), Early warning of summer drought over Texas and the south central United States: Spring conditions as a harbinger of summer drought, *Rep. Texas Water Development Board Tech. Note15-02*, Texas Water Development Board.

Hoerling, M., and A. Kumar (2003), The perfect ocean for drought, *Science*, *299*(5607), 691–694, doi:10.1126/science.1079053.

Jones, P., and I. Harris (2013), CRU TS3.21: Climatic Research Unit (CRU) time-series (TS) version 3.21 of high resolution gridded data of month-by-month variation in climate (Jan. 1901–Dec. 2012), NCAS British Atmos. Data Centre.

Kalnay, E., et al. (1996), The NCEP/NCAR 40-year reanalysis project, *Bull. Am. Meteorol. Soc.*, *77*(3), 437–471, doi:10.1175/1520-0477(1996)077<0437:Tnyrp>2.0.Co;2.

Krishnamurthy, L., G. A. Vecchi, R. Msadek, A. Wittenberg, T. L. Delworth, and A. F. Zeng (2015), The seasonality of the Great Plains low-level jet and ENSO relationship, *J. Clim.*, *28*, 4525–4544.

Kushnir, Y., R. Seager, M. F. Ting, N. Naik, and J. Nakamura (2010), Mechanisms of tropical Atlantic SST influence on North American precipitation variability, *J. Clim.*, *23*(21), 5610–5628, doi:10.1175/2010jcli3172.1.

Lau, N. C., A. Leetmaa, and M. J. Nath (2006), Attribution of atmospheric variations in the 1997–2003 period to SST anomalies in the Pacific and Indian Ocean Basins, *J. Clim.*, *19*(15), 3607–3628, doi:10.1175/Jcli3813.1.

Liu, A. Z., M. F. Ting, and H. L. Wang (1998), Maintenance of circulation anomalies during the 1988 drought and 1993 floods over the United States, *J. Atmos. Sci.*, *55*(17), 2810–2832, doi:10.1175/1520-0469(1998)055<2810:Mocadt>2.0.Co;2.

Magaña, V., J. A. Amador, and S. Medina (1999), The midsummer drought over Mexico and Central America, *J. Clim.*, *12*(6), 1577–1588, doi:10.1175/1520-0442(1999)012<1577:Tmdoma>2.0.Co;2.

Mo, K. C., J. K. E. Schemm, and S. H. Yoo (2009), Influence of ENSO and the Atlantic multidecadal oscillation on drought over the United States, *J. Clim.*, *22*(22), 5962–5982, doi:10.1175/2009jcli2966.1.

Nigam, S., B. Guan, and A. Ruiz-Barradas (2011), Key role of the Atlantic Multidecadal Oscillation in 20th century drought and wet periods over the Great Plains, *Geophys. Res. Lett.*, *38*, L16713, doi:10.1029/2011GL048650.

Rayner, N. A., D. E. Parker, E. B. Horton, C. K. Folland, L. V. Alexander, D. P. Rowell, E. C. Kent, and A. Kaplan (2003), Global analyses of sea surface temperature, sea ice, and night marine air temperature since the late nineteenth century, *J. Geophys. Res.*, *108*(D14), 4407, doi:10.1029/2002JD002670.

Ruiz-Barradas, A., and S. Nigam (2005), Warm season rainfall variability over the US great plains in observations, NCEP and ERA-40 reanalyses, and NCAR and NASA atmospheric model simulations, *J. Clim.*, *18*(11), 1808–1830, doi:10.1175/Jcli3343.1.

Schubert, S., et al. (2009), A US CLIVAR project to assess and compare the responses of global climate models to drought-related SST forcing patterns: Overview and results, *J. Clim.*, *22*(19), 5251–5272, doi:10.1175/2009jcli3060.1.

Schubert, S. D., M. J. Suarez, P. J. Pegion, R. D. Koster, and J. T. Bacmeister (2004), Causes of long-term drought in the US Great Plains, *J. Clim.*, *17*(3), 485–503, doi:10.1175/1520-0442(2004)017<0485:Coldit>2.0.Co;2.

Seager, R. (2007), The turn of the century North American drought: Global context, dynamics, and past analogs, *J. Clim.*, *20*(22), 5527–5552, doi:10.1175/2007JCLI1529.1.

Seager, R., and M. Hoerling (2014), Atmosphere and ocean origins of North American droughts, *J. Clim.*, *27*(12), 4581–4606, doi:10.1175/Jcli-D-13-00329.1.

Seager, R., N. Harnik, Y. Kushnir, W. Robinson, and J. Miller (2003), Mechanisms of hemispherically symmetric climate variability, *J. Clim.*, *16*(18), 2960–2978, doi:10.1175/1520-0442(2003)016<2960:Mohscv>2.0.Co;2.

Seager, R., N. Harnik, W. A. Robinson, Y. Kushnir, M. Ting, H. P. Huang, and J. Velez (2005a), Mechanisms of ENSO-forcing of hemispherically symmetric precipitation variability, *Q. J. R. Meteorol. Soc.*, *131*(608), 1501–1527, doi:10.1256/Qj.04.96.

Seager, R., Y. Kushnir, C. Herweijer, N. Naik, and J. Velez (2005b), Modeling of tropical forcing of persistent droughts and pluvials over western North America: 1856–2000, *J. Clim.*, *18*(19), 4065–4088, doi:10.1175/Jcli3522.1.

Seager, R., M. Ting, M. Davis, M. Cane, N. Naik, J. Nakamura, C. Li, E. Cook, and D. W. Stahle (2009), Mexican drought: An observational modeling and tree ring study of variability and climate change, *Atmosfera*, *22*(1), 1–31.

Seager, R., L. Goddard, J. Nakamura, N. Henderson, and D. E. Lee (2014), Dynamical causes of the 2010/11 Texas-Northern Mexico Drought*, *J. Hydrometeorol.*, *15*(1), 39–68, doi:10.1175/Jhm-D-13-024.1.

Smith, T. M., R. W. Reynolds, T. C. Peterson, and J. Lawrimore (2008), Improvements to NOAA's historical merged land-ocean surface temperature analysis (1880–2006), *J. Clim.*, *21*(10), 2283–2296.

Ting, M. F., and H. Wang (1997), Summertime US precipitation variability and its relation to Pacific sea surface temperature, *J. Clim.*, *10*(8), 1853–1873, doi:10.1175/1520-0442(1997)010<1853:Suspva>2.0.Co;2.

Trenberth, K. E., G. W. Branstator, and P. A. Arkin (1988), Origins of the 1988 North-American drought, *Science*, *242*(4886), 1640–1645, doi:10.1126/science.242.4886.1640.

Wang, H., A. Kumar, W. Wang, and B. Jha (2012), U.S. summer precipitation and temperature patterns following the peak phase of El Niño, *J. Clim.*, *25*, 7204–7215.

Weaver, S. J., and S. Nigam (2008), Variability of the great plains low-level jet: Large-scale circulation context and hydroclimate impacts, *J. Clim.*, *21*(7), 1532–1551, doi:10.1175/2007jcli1586.1.

Weaver, S. J., S. Schubert, and H. Wang (2009), Warm season variations in the low-level circulation and precipitation over the central United Sates in observations, AMIP simulations, and idealized SST experiments, *J. Clim.*, *22*, 5401–5420, doi:10.1175/2009JCLI2984.1.

Worster, D. (1979), *Dust Bowl: The Southern Plains in the 1930s*, 277 pp., Oxford Univ. Press, New York.